Since January 2020 Elsevier has created a COVID-19 resource centre with free information in English and Mandarin on the novel coronavirus COVID-19. The COVID-19 resource centre is hosted on Elsevier Connect, the company's public news and information website.

Elsevier hereby grants permission to make all its COVID-19-related research that is available on the COVID-19 resource centre - including this research content - immediately available in PubMed Central and other publicly funded repositories, such as the WHO COVID database with rights for unrestricted research re-use and analyses in any form or by any means with acknowledgement of the original source. These permissions are granted for free by Elsevier for as long as the COVID-19 resource centre remains active.

Journal Pre-proof

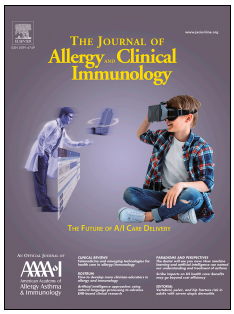

The OM-85 bacterial lysate inhibits SARS-CoV-2 infection of epithelial cells by downregulating SARS-CoV-2 receptor expression

Vadim Pivniouk, PhD, Oksana Pivniouk, MA, Avery DeVries, PhD, Jennifer L. Uhrlaub, MS, Ashley Michael, BS, Denis Pivniouk, BS, Sydney R. VanLinden, BS, Michelle Y. Conway, BS, Seongmin Hahn, MS, Sean P. Malone, Peace Ezeh, PhD, Jared M. Churko, PhD, Dayna Anderson, BS, Monica Kraft, MD, Janko Nikolich-Zugich, MD, PhD, Donata Vercelli, MD

PII: S0091-6749(21)02581-1

DOI: https://doi.org/10.1016/j.jaci.2021.11.019

Reference: YMAI 15381

To appear in: *Journal of Allergy and Clinical Immunology*

Received Date: 11 May 2021

Revised Date: 14 November 2021

Accepted Date: 19 November 2021

Please cite this article as: Pivniouk V, Pivniouk O, DeVries A, Uhrlaub JL, Michael A, Pivniouk D, VanLinden SR, Conway MY, Hahn S, Malone SP, Ezeh P, Churko JM, Anderson D, Kraft M, Nikolich-Zugich J, Vercelli D, The OM-85 bacterial lysate inhibits SARS-CoV-2 infection of epithelial cells by downregulating SARS-CoV-2 receptor expression, *Journal of Allergy and Clinical Immunology* (2022), doi: https://doi.org/10.1016/j.jaci.2021.11.019.

This is a PDF file of an article that has undergone enhancements after acceptance, such as the addition of a cover page and metadata, and formatting for readability, but it is not yet the definitive version of record. This version will undergo additional copyediting, typesetting and review before it is published in its final form, but we are providing this version to give early visibility of the article. Please note that, during the production process, errors may be discovered which could affect the content, and all legal disclaimers that apply to the journal pertain.

© 2021 Published by Elsevier Inc. on behalf of the American Academy of Allergy, Asthma & Immunology.

The OM-85 bacterial lysate inhibits SARS-CoV-2 infection of epithelial cells by downregulating SARS-CoV-2 receptor expression

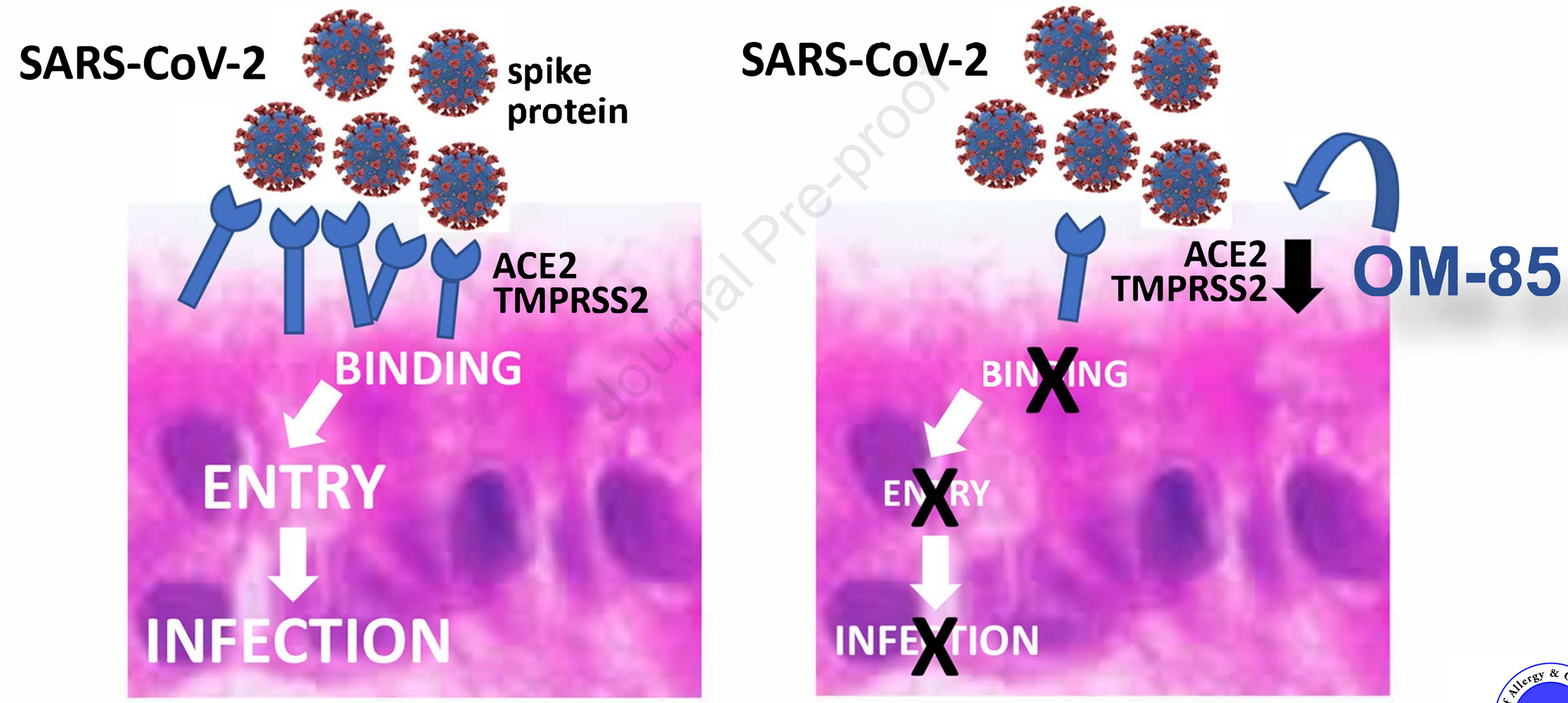

Journal Pre-proof

The OM-85 bacterial lysate inhibits SARS-CoV-2 infection of epithelial cells by downregulating SARS-CoV-2 receptor expression

Vadim Pivniouk, PhD[1,2,3], Oksana Pivniouk, MA[2], Avery DeVries, PhD[2,3], Jennifer L. Uhrlaub, MS[4], Ashley Michael, BS[2], Denis Pivniouk, BS, Sydney R. VanLinden, BS[2], Michelle Y. Conway, BS[5], Seongmin Hahn, MS[2], Sean P. Malone[2], Peace Ezeh, PhD[2], Jared M. Churko, PhD[1,3], Dayna Anderson, BS[2], Monica Kraft, MD[3,5], Janko Nikolich-Zugich, MD, PhD[3,4], and Donata Vercelli, MD[1,2,3,6]

[1]Department of Cellular and Molecular Medicine, The University of Arizona, Tucson, AZ, 85721, USA

[2]Asthma and Airway Disease Research Center, The University of Arizona, Tucson, AZ, 85721, USA

[3]The BIO5 Institute, The University of Arizona, Tucson, AZ, 85721, USA

[4]Department of Immunobiology, The University of Arizona, Tucson, AZ, 85721, USA

[5]Department of Medicine, The University of Arizona, Tucson, AZ, 85721, USA

[6]Arizona Center for the Biology of Complex Diseases, The University of Arizona, Tucson, AZ, 85721, USA

Corresponding author: Donata Vercelli, MD, The University of Arizona, 1657 E. Helen St., Tucson, AZ 85721, Phone: (520) 626-6387, E-mail: donata@arizona.edu

Conflict of Interest:

This work was funded in part by a research grant provided by OM Pharma SA to the University of Arizona. Support was also provided by post-doctoral fellowships from T32

Journal Pre-proof

ES007091 and The BIO5 Institute (to ADV), a pre-doctoral T32 HL007249 fellowship (to SRVL), and P01AI148104, R21AI144722 and R25HL126140 (to DV).

DV and VP are inventors in PCT/EP2019/074562, “Method of Treating and/or Preventing Asthma, Asthma Exacerbations, Allergic Asthma and/or Associated Conditions with Microbiota Related to Respiratory Disorders”. M.K has received grants from NIH, ALA, Chiesi, Sanofi, Astra-Zeneca, speaker fees from Chiesi outside this work and consulting fees from Astra-Zeneca and Sanofi, outside the submitted work. J.N.Ž. is co-chair of the scientific advisory board of and receives research funding from Young Blood Institute, Inc. All other authors have nothing to disclose.

Journal Pre-proof

ABSTRACT

Background Treatments for coronavirus disease of 2019 (COVID-19), which is caused by severe acute respiratory syndrome coronavirus-2 (SARS-CoV-2), are urgently needed but remain limited. SARS-CoV-2 infects cells through interactions of its spike (S) protein with ACE2 and TMPRSS2 on host cells. Multiple cells and organs are targeted, particularly airway epithelial cells. OM-85, a standardized lysate of human airway bacteria with strong immunomodulating properties and an impeccable safety profile, is widely used to prevent recurrent respiratory infections. We found that airway OM-85 administration inhibits *Ace2* and *Tmprss2* transcription in the mouse lung, suggesting that OM-85 might hinder SARS-CoV-2/host cell interactions.

Objectives To investigate whether and how OM-85 treatment protects non-human primate and human epithelial cells against SARS-CoV-2.

Methods *ACE2* and *TMPRSS2* mRNA and protein expression, cell binding of SARS-CoV-2 S1 protein, cell entry of SARS-CoV-2 S protein-pseudotyped lentiviral particles, and SARS-CoV-2 cell infection were measured in kidney, lung and intestinal epithelial cell lines, primary human bronchial epithelial cells, and *ACE2*-transfected HEK293T cells treated with OM-85 *in vitro.*

Results OM-85 significantly downregulated *ACE2* and *TMPRSS2* transcription and surface ACE2 protein expression in epithelial cell lines and primary bronchial epithelial cells. OM-85 also strongly inhibited SARS-CoV-2 S1 protein binding to, SARS-CoV-2 S protein-pseudotyped lentivirus entry into, and SARS-CoV-2 infection of epithelial cells.

Journal Pre-proof

These effects of OM-85 appeared to depend on SARS-CoV-2 receptor downregulation.

Conclusion OM-85 inhibits SARS-CoV-2 epithelial cell infection *in vitro* by downregulating SARS-CoV-2 receptor expression. Further studies are warranted to assess whether OM-85 may prevent and/or reduce the severity of COVID-19.

Journal Pre-proof

KEY MESSAGES

- The OM-85 bacterial lysate downregulates the SARS-CoV-2 receptor *ACE2* and *TMPRSS2* in epithelial cells and strongly inhibits SARS-CoV-2 S-1 protein binding to, SARS-CoV-2 S protein-pseudotyped lentivirus entry into, and SARS-CoV-2 infection of these cells.

- The ability of OM-85 to inhibit SARS-CoV-2 infection of epithelial cells *in vitro* and its excellent safety profile warrant further studies of its effects against COVID-19.

CAPSULE SUMMARY

The OM-85 bacterial lysate inhibits multiple steps in SARS-CoV-2 epithelial cell infection *in vitro*. These properties, and the excellent safety profile of OM-85, warrant further studies of its effects against COVID-19.

Journal Pre-proof

KEY WORDS

COVID-19

SARS-CoV-2

Bacterial lysate

OM-85

Epithelial cells

ACE2

TMPRSS2

ABBREVIATIONS

ACE2	angiotensin-converting enzyme 2
COVID-19	coronavirus disease of 2019
CMV	cytomegalovirus
ELISA	enzyme-linked immunosorbent assay
GAPDH	glyceraldehyde 3-phosphate dehydrogenase
GFP	green fluorescent protein
i.n.	intranasal
MFI	mean fluorescence intensity
NHP	non-human primate

Journal Pre-proof

90	PE	phycoerythrin
91	PFU	plaque forming units
92	RT-qPCR	reverse transcription quantitative polymerase chain reaction
93	SARS-CoV-2	severe acute respiratory syndrome coronavirus-2
94	S	spike
95	TMPRSS2	transmembrane protease serine 2
96	TU	transducing units
97	VSV	vesicular stomatitis virus
98	WT	wild-type

Journal Pre-proof

Introduction

The emergence of severe acute respiratory syndrome coronavirus-2 (SARS-CoV-2) in December 2019 triggered a global pandemic marked by a broad spectrum of clinical manifestations. These range from a mild, self-limiting flu-like respiratory illness to life-threatening multi-organ failure and are collectively referred to as coronavirus disease of 2019 (COVID-19)[1, 2]. Angiotensin-converting enzyme 2 (ACE2) on host cells serves as the main receptor for SARS-CoV-2 spike (S) protein attachment[3-5], while the endogenous transmembrane protease serine 2 (TMPRSS2) cleaves the S protein, thus allowing fusion of viral and cellular membranes[3]. These events promote efficient viral entry and productive infection of target cells. *ACE2* and *TMPRSS2* are expressed in several tissues and in multiple airway epithelial cell types, particularly nasal[6] and alveolar type II cells, goblet cells and ciliated cells[7]. While the receptor expression pattern and aerosol mode of transmission[8] of SARS-CoV-2 render the airways a primary viral target, kidney and intestinal epithelial cells also express *ACE2* and *TMPRSS2* and can become infected in patients[9, 10].

Despite rapid progress in our understanding of COVID-19 pathogenesis, treatment options for this disease remain limited. Although several vaccines are being deployed, inoculating the world population will require much time, and the emergence of viral mutants with decreased sensitivity to vaccines remains a distinct possibility[11]. Novel, safe and accessible strategies to reduce the frequency and/or severity of SARS-CoV-2 infection are therefore highly desirable. Oral administration of OM-85 (Broncho-Vaxom™), a standardized lysate of 21 bacterial strains often found in the human

airways[12], is widely used empirically in Europe, South America and Asia for the prophylaxis of upper airway recurrent infections in adults[12] and children[13], with an excellent safety profile[14]. An NIH-sponsored trial (NCT02148796) is currently ongoing in the United States, where OM-85 is not yet approved. The trial is testing whether oral administration of the lysate prevents wheezing lower respiratory illnesses or asthma-like symptoms in young high-risk children. The mechanisms underlying OM-85-mediated protection from respiratory infections are complex[15, 16] and remain incompletely understood. We recently found that OM-85 boosts human airway epithelial cell barrier function *in vitro* and regulates multiple airway barrier-related transcriptional networks in the lung following intranasal (i.n.) administration to mice[17]. These findings prompted us to investigate whether OM-85 also affects the expression of genes involved in SARS-CoV-2 infection of epithelial cells.

Journal Pre-proof

Methods

Cell lines and primary airway epithelial cells The Vero E6 African green monkey (*Chlorocebus sabaeus*) kidney-derived cell line was kindly provided by Dr. M. Kraft (University of Arizona). Calu-3 human lung cells and HEK293T/17 cells (HTB55™ and CRL-11268™, respectively) were purchased from ATCC (Manassas, VA). Caco-2 human colon cells were a kind gift from Dr. J. Wilson (University of Arizona). HEK293T cells stably expressing human *ACE2* were purchased from GeneCopoeia (Rockville, MD). All cell lines were propagated in Dulbecco's modified Eagle medium (DMEM) (Gibco, Thermo Fisher Scientific, Waltham, MA) supplemented with FBS (10%, Sigma, St. Louis, MO), GlutaMax (2 mM), penicillin (50 units/ml) and streptomycin (50 μg/ml, all from Gibco). Vero cells for SARS-CoV-2 infection experiments were obtained from ATCC (CCL-81).

To obtain human primary airway cells, participants were recruited from the population in Tucson, Arizona and the surrounding areas. Before undergoing any procedure, informed consent according to an Institutional Review Board-approved protocol was obtained from each participant. Healthy participants had no evidence of airway obstruction and no history of pulmonary disease; atopy (as determined by clinical history, allergen skin testing and blood eosinophil levels) was not an exclusion criterion. Participants underwent bronchoscopy with endobronchial-protected brushing, as previously described[18]. To obtain bronchial epithelial cells, brushing of the proximal airways was performed using a separate protected cytologic brush for each pass, for a total of ten passes. Participants were discharged after their forced expiratory volume in 1 second reached 90% of their pre-bronchoscopy, post-albuterol value.

Journal Pre-proof

Freshly isolated airway bronchial epithelial cells from endobronchial brushing were cultured with PneumaCult™-EX Plus Medium (StemCell Technologies, Vancouver, British Columbia, Canada). Once confluent, cells were trypsinized and seeded onto collagen-coated polyester 12-mm-diameter Transwell™ insert membranes (Corning, Waltham, MA) at $4x10^4$ cells/well. To allow for differentiation, cells were cultured at air–liquid interface for 2 weeks with PneumaCult™ -Air-Liquid Interface Medium (StemCell Technologies).

Plasmids The lentiviral packaging plasmid, psPAX2, and the VSV-G envelope expressing plasmid, pMD2.G, (Addgene plasmid # 12260; http://n2t.net/addgene:1226; RRID:Addgene_12260, and Addgene plasmid # 12259; http://n2t.net/addgene:12259; RRID:Addgene_12259) were gifts from Didier Trono (École Polytechnique Fédérale de Lausanne, Switzerland). The lentiviral reporter plasmid pCIB-GFP expressing GFP was kindly provided by Dr. Michael Johnson (University of Arizona). The SARS-CoV-2 Spike protein expressing plasmid HDM-SARS2-Spike-delta21 (Addgene plasmid # 155130; http://n2t.net/addgene:155130; RRID:Addgene_155130)[19] was a gift from Jesse Bloom (University of Washington, Seattle, WA).

Functional S1 protein binding assay Cells were grown in 6- or 12-well plates until confluent and treated with OM-85 (0.12, 0.24, 0.48, 0.96, or 1.92 mg/ml) or PBS. After 72 hours, cells were harvested, washed and resuspended in FACSWash buffer (PBS with 1% BSA and 0.1% NaN_3) at $0.5\text{-}1x10^7$ cells/ml. To block nonspecific staining, cells were incubated on ice for 10 min in the same buffer containing normal rat serum (2%) followed by a 30 min incubation with recombinant His-tagged S1 protein (5.625 μg/ml:

Sino Biological US, Wayne, PA). After an additional 30 min incubation with an anti-His tag-PE antibody (Cat# 362603, Biolegend, San Diego, CA), cells were washed with FACSWash buffer and analyzed by flow cytometry. At least 20,000 events were acquired on an LSR II or a FACSCalibur flow cytometer (BD Biosciences) and analyzed with FlowJo software (Version 10.6.0, Becton Dickinson, 2019). S1 binding was expressed as the percentage of S1-binding cells in each sample relative to the average of PBS-treated samples.

Production of pseudotyped lentiviral particles HEK 293T/17 cells were transfected overnight in 100 mm dishes with packaging plasmid psPAX2 (15 μg) plus envelope plasmids (either HDM-SARS2-Spike-delta21 or pMD2.G: 15 μg) and HIV reporter plasmid expressing GFP (pCIB-GFP: 15 μg) using Lipofectamine 3000 (ThermoFisher Scientific) according to the manufacturer's instructions. The next day, the transfection medium was replaced with fresh complete DMEM. Virus-containing supernatants were collected 48 hours later and kept frozen at -80ºC. The concentration of viral particles was estimated using an HIV p24 ELISA (Abcam, Cambridge, MA). The functional titer of VSV-G-pseudotyped lentivirus (positive control), i.e., the number of virions capable of productively integrating into cells per ml of viral preparation, was determined by flow cytometry quantification of GFP^+ Vero E6 cells as described[20, 21] and was estimated to be 2.34×10^6 transducing units (TU)/ml. The titer of SARS-CoV-2-S protein-pseudotyped virus was estimated to be 1×10^4 TU/ml through side-by-side comparison with serial dilutions of VSV-G-pseudotyped lentivirus in Vero E6 cells.

Cell transduction with pseudotyped viral particles Cells were cultured in 24- or 96-

well plates until confluent and then treated with OM-85 (0.48 mg/ml). After 48 hours, the OM-85-containing medium was replaced with medium that was supplemented with polybrene (6 μg/ml) and contained either SARS-CoV-2 S protein- ($2x10^3$ TU) or VSV-G protein- ($2.34x10^4$ TU) pseudotyped lentivirus. Plates were centrifuged at 2,000x*g* for 1 hour at room temperature and cultured overnight at 37°C in a 5% CO_2 atmosphere. The GFP fluorescence generated upon transcription and translation of the reporter gene by transduced cells was assessed 72 hours post-transduction using an Axio Vert microscope (Carl Zeiss Microscopy, White Plains, NY) under 10x magnification. At least 20 (SARS-CoV-2-pseudotyped virus) or 10 (VSV-G-pseudotyped virus) frames/well were recorded using an Axiocam 305 camera (Carl Zeiss Microscopy) and quantified by counting fluorescent pixels with the Slide Analyzer software (https://github.com/dpivniouk/slide_analyzer).

SARS-CoV-2 infection SARS-CoV-2, isolate USA-WA1/2020, was deposited by Dr. Natalie J. Thornburg at the Centers for Disease Control and Prevention and obtained from the World Reference Center for Emerging Viruses and Arboviruses (WRCEVA). Stocks of SARS-CoV-2 were generated as a single passage from received stock vial on mycoplasma-negative Vero cells (ATCC CCL-81).

For the virus inhibition assay, preliminary flow cytometry experiments established that OM-85 stimulation decreased S1 protein binding to Vero cells (ATCC CCL-81) to levels comparable to those seen in Vero E6 cells (not shown). Vero cells ($1x10^6$ per 96-well, flat bottom plate) were pretreated with PBS or increasing OM-85 concentrations (0.24-1.92 mg/ml) for a total of 72 or 96 hours. Twenty-four hours prior to adding SARS-CoV-

2, cells were dissociated with 0.25% trypsin, washed once with media in the original plate, and re-plated from one to three 96-well plates; OM-85 was replenished at the original concentrations. At the 72- or 96-hour treatment time point, SARS-CoV-2 (15 plaque forming units, pfu/well) was added in the presence or absence of OM-85. The virus was incubated for 2 hours to allow infection of the monolayer and then dumped off. Cells were then overlayed with 1% methylcellulose in 5% DMEM without OM-85. Four days later, plates were fixed in 10% Neutral Buffered Formalin for 30 minutes and stained with 1% crystal violet. Plaques were imaged using an ImmunoSpot Versa plate reader (Cellular Technology Limited, Cleveland, OH) and counted. Results were expressed as average numbers of pfus/well detected in quadruplicate wells for each condition.

Calu-3 cells were plated at $0.5x10^6$ per 96-well plate for 24 hours and then treated with PBS or OM-85 (0.24-1.92 mg/ml). After 72 hours, the medium was removed and SARS-CoV-2 (WA/2020, ~100 pfu) was added to all wells. After 2 hours, the virus was removed and replaced with fresh medium containing the original OM-85 concentrations; cells were then cultured for 48 additional hours. Plates were then frozen at -80^{o}C to release virus and centrifuged to pellet debris. To determine viral titers in Calu-3 cultures, virus-containing supernatants from each row of a Calu-3 plate were titrated by 10-fold serial dilutions on 96-well indicator Vero plates and incubated for 2 hours. Indicator Vero plates were then overlayed with 1% methylcellulose in fresh medium and incubated for 4 days to allow plaques to develop. Plates were fixed and stained as above, and plaques were counted. The number of pfus/well of Calu-3 plates was calculated by dividing the number of plaques on indicator Vero plates by the dilution factor. Results

were expressed as average numbers of pfus/well detected in 8 replicates from the original Calu-3 plate.

OM-85 preparations and all other experimental procedures and statistical methods are detailed in the Online Repository.

Journal Pre-proof

Results

OM-85 inhibits Ace2 and Tmprss2 transcription in the mouse lung through the Myd88/Trif pathway Our recent studies assessing how OM-85 administration to the airway compartment affects immune responses in the mouse lung[17] provided the first clue that OM-85 might affect SARS-CoV-2/host interactions. RNA-seq profiling of the lung transcriptome in Balb/c mice treated i.n. with OM-85 according to an optimized protocol (1 mg/treatment x 14 treatments over 32 days, with terminal assessments at day 39: **Fig.1A**) identified multiple genetic networks regulated by the lysate. Especially notable was the upregulation of signature genes related to tight junctions and epithelial barrier function[17]. Interestingly, a preliminary analysis focused on the expression of the SARS-CoV-2 receptors *Ace2* and *Tmprss2* revealed a nominally significant (p=0.02) inhibition of *Ace2* expression in OM-85-treated mice compared to PBS-treated controls. *Tmprss2* expression was also decreased, albeit not significantly (**Fig. 1B**). RT-qPCR with *Ace2*- and *Tmprss2*-specific primers was then used to measure lung expression of these genes and compare their mRNA levels at day 34 and 39 of our protocol (i.e., 2 and 7 days after the last OM-85 treatment: **Fig. 1A**). We chose the 7-day time point because it was optimal for inhibition of experimental allergic asthma and was used to generate the RNA-seq data presented here[17]. On the other hand, the 2-day time point allowed us to explore shorter-term effects. Relative to PBS-treated mice, *Tmprss2* was significantly downregulated at both time points (P=0.01 and P=0.003, respectively: **Fig. 1D**), whereas *Ace2* was significantly (P=0.01) inhibited only at the earlier time point (**Fig. 1C**). These experiments showed that delivery of OM-85 to the airways affected the expression of the major SARS-CoV-2 receptor components in the lung, with distinct

time-dependent effects.

Because OM-85 is a bacterial lysate whose ability to protect from asthma *in vivo* depends on Myd88/Trif innate immune signaling[17], we then assessed whether OM-85-induced inhibition of *Ace2* and *Tmprss2* transcription in the mouse lung also required this pathway. These experiments, which were performed in C57BL/6 mice, revealed that as few as four i.n. treatments with OM-85 (1 mg/treatment: **Fig. E1A**) were sufficient to reduce *Ace2* and *Tmprss2* expression by 59% and 63%, respectively, in lung cells isolated from wild-type (WT) mice. In contrast, negligible changes in the expression of these genes were detected in *Myd88*$^{-/-}$*Trif*$^{-/-}$ mice (**Fig. E1B**). These findings indicated that OM-85-induced downregulation of *Ace2* and *Tmprss2* transcription in mouse lung tissue is *Myd88/Trif*-dependent and strain-independent.

OM-85 inhibits Ace2 and Tmprss2 expression in non-human primate (NHP) and human epithelial cells in vitro Our initial results illustrated the *in vivo* effects of OM-85 in the airways, a main target of SARS-CoV-2. However, further mechanistic dissections in these models were problematic because lung *Ace2* and *Tmprss2* expression likely derived from multiple cell types[7, 22]. Moreover, mice are not naturally susceptible to infection by most SARS-CoV-2 strains[23]. Therefore, subsequent experiments relied on RT-qPCR to assess the effects of OM-85 on *ACE2* and *TMPRSS2* expression in NHP Vero E6 as well as human Calu-3 and Caco-2 epithelial cells. These cells derive from SARS-CoV-2 target organs (kidney, lung and colon, respectively) of naturally susceptible species[23] and thus provide ideal models to characterize the interactions of epithelial cells with, and their infection by, SARS-CoV-2[3, 4, 24-26]. OM-85 (0.48 mg/ml) significantly and strongly inhibited *ACE2* expression in

Journal Pre-proof

kidney Vero E6 cells after 24 and 48 hours of stimulation (P=0.00004 and P=0.0006, respectively: **Fig. 2A**). *TMPRSS2* was also significantly decreased at the same time points (P=0.0002 and P=0.01, respectively: **Fig. 2B**). In contrast, *ACE2* expression by lung Calu-3 cells was significantly inhibited only after 72 and 96 hours, and only when fresh OM-85 was replaced after 48 hours of culture (P=0.009 and P=0.002, respectively: **Fig. 2C**). *TMPRSS2* expression was inhibited at the 24-hour time point (P=0.02) as well as at 72 and 96 hours, but only when at 48 hours spent medium was replaced with fresh medium containing the original concentration of OM-85 (P=0.03 and P=0.01, respectively: **Fig. 2D**). Therefore, OM-85 inhibited expression of both *ACE2* and *TMPRSS2* in Vero E6 and Calu-3 epithelial cells, but overall downregulation occurred more rapidly in the former than in the latter. A 48-hour stimulation with OM-85 (0.48 mg/ml) also significantly reduced *ACE2* and *TMPRSS2* mRNA levels in intestinal Caco-2 cells (P=0.01 and P=0.003, respectively: **FIG. E2**).

To further explore the significance of our findings, we turned to human primary airway cells, a pre-eminent natural SARS-CoV-2 target. Bronchial epithelial cells isolated from a healthy individual were differentiated at the air–liquid interface for 2 weeks. *ACE2* and *TMPRSS2* mRNA levels were then measured by RT-qPCR after a 48- or 72-hour incubation with PBS or OM-85 (1.92 mg/ml). **Fig. 3** shows strong, significant inhibition of *ACE2* at 48 and 72 hours (P=0.01 and P=0.005, respectively) and a more modest, but still significant inhibition of *TMPRSS2* at 72 hours (P=0.04). These results from OM-85-treated human normal primary epithelial cells overall validated those generated in epithelial cell lines.

Journal Pre-proof

We next assessed whether decreased SARS-CoV-2 receptor transcription was associated with reduced surface levels of receptor protein. To this end, Vero E6 and Calu-3 cells were incubated with PBS or OM-85 (0.48 and 1.92 mg/ml) for 72 hours and examined by flow cytometry with ACE2-specific monoclonal antibodies. OM-85 treatment significantly and dose-dependently decreased both ACE2 mean fluorescence intensity (MFI) (P=0.002 and P=0.0002, respectively) and the percentage of ACE2-positive cells in Vero E6 cells **(Fig. 4A-C)** and Calu-3 cells (P=0.005 for ACE2 MFI and ACE2-positive cell percentages at 1.92 mg/ml: **Fig. 4D-F)**. In combination, these results demonstrate that *in vitro* stimulation with the OM-85 bacterial lysate dampens SARS-CoV-2 receptor expression on epithelial cells from distinct organs.

OM-85 reduces S1 protein-mediated attachment to epithelial cells Because ACE2 and TMPRSS2 enable SARS-CoV-2 infection of epithelial cell by mediating S protein attachment to, and viral entry into these cells, we next investigated whether OM-85-induced downregulation of *ACE2* and *TMPRSS2* interferes with these processes. To assess the effects of OM-85 on SARS-CoV-2 S protein attachment, we developed an S1 protein binding assay. Cells were incubated with a recombinant His-tagged S1 subunit comprising the SARS-CoV-2 receptor binding domain[3], followed by a phycoerythrin (PE)-conjugated anti-His antibody. S1 protein binding to cells was assessed by flow cytometry. We validated the ability of this assay to specifically detect ACE2-mediated S1 protein cellular binding using HEK293T cells, untransfected or stably transfected with human *ACE2* (ACE2/HEK293T). S1 binding was detected in only 5% of untransfected HEK293T cells and ACE2/HEK293T cells incubated with anti-His-

Journal Pre-proof

PE antibody without S1 protein, while >99% of PBS-treated ACE2/HEK293T cells bound S1 protein (**Fig. 5A**).

Using this S1 protein binding assay, we then found that a substantial proportion of Vero E6 (22 ± 0.5%) and Calu-3 (24 ± 1%) epithelial cells bound SARS-CoV-2 S1 protein (**Fig. 5B**). Preliminary dose-response curves with a broad range of OM-85 concentrations (0.12 to 1.92 mg/ml) showed dose-dependent inhibition of S1 binding to Vero E6 cells, with significant effects (P=7.00E-07) even at the lowest concentration (0.12 mg/ml) and robust inhibition at concentrations ≥ 0.48 mg/ml **(Fig. E3**). A 72-hour incubation with OM-85 (0.48 or 1.92 mg/ml) dose-dependently reduced S1 binding by 42 ± 4% (P=8E-05) and 53 ± 1.3% (P=1E-10) for Vero E6 cells, and 29 ± 5.6**%** (P=0.009) and 71 ± 2.3**%** (P=6E-05) for Calu-3 cells (**Fig. 5C**).

These results demonstrated that OM-85 efficiently inhibited S1 protein attachment to epithelial cells derived from natural SARS-CoV-2 target organs. Mechanistically, our findings strongly suggested that this inhibition reflected OM-85-dependent interference with the physiologic regulation of *ACE2* expression. In support of this notion, even a maximal concentration of OM-85 (1.92 mg/ml) failed to inhibit ACE2 protein expression on (**Table E1**), and S1 protein binding to (**Fig. 5A, right**), ACE2/HEK293T cells in which human *ACE2* transcription is driven by a heterologous, OM-85-unresponsive cytomegalovirus promoter.

OM-85 inhibits the entry of S protein-pseudotyped lentiviral particles into epithelial cells To investigate whether OM-85-dependent inhibition of SARS-CoV-2 receptor expression in, and SARS-CoV-2 S1 protein attachment to, epithelial cells also

reduces S protein-mediated SARS-CoV-2 entry into these cells, we directly measured the entry of replication-deficient, SARS-CoV-2 S protein-pseudotyped lentiviral particles into epithelial cells pre-incubated with OM-85 or PBS. Our lentiviral particles carried a GFP reporter gene that is transcribed and translated by transduced cells, and were pseudotyped with SARS-CoV-2 S protein or the G glycoprotein of the pantropic vesicular stomatitis virus (VSV: positive transduction control)[3]. As expected, VSV-G-pseudotyped particles efficiently transduced Vero E6 cells, with functional titers reaching $2.3x10^6$ transducing units (TU)/ml (**Fig. 6A**, **top right**). Vero E6 transduction by SARS-CoV-2-pseudotyped particles was less efficient but still robust and consistent (**Fig. 6A**, **top left**), with titers reaching $1x10^4$ TU/ml.

OM-85 pre-treatment (0.48 mg/ml) strongly (P=2.5E-05) inhibited SARS-CoV-2 S protein-mediated Vero E6 cell transduction (**Fig. 6A, left**, and **Fig. 6B**). This effect was specific because transduction by VSV-G-pseudotyped particles remained unaffected (**Fig. 6A, right**, and **Fig. 6C**). The effects of OM-85 on viral entry into Calu-3 cells could not be reliably estimated because these cells were poorly transduced under our experimental conditions. Indeed, both percentages of GFP^+ cells and GFP MFI in these cells were consistently low following transduction with either SARS-CoV-2 S protein- or VSV-G (positive control) pseudotyped particles (not shown). Notably, ACE2/HEK293T cells were readily transduced by both SARS-CoV-2 S- and VSV-G-pseudotyped viral particles, but OM-85 failed to inhibit viral entry into these cells (**Fig. 6D-E**). Because ACE2/HEK293T cells do not downregulate *ACE2* upon OM-85 stimulation (**Table E1**), these findings were consistent with the notion that OM-85-induced suppression of events leading to SARS-CoV-2 infection involves a reduction of *ACE2* expression.

OM-85 inhibits SARS-CoV-2 infection of epithelial cells from distinct tissues The data discussed above had shown that OM-85 effectively inhibits both SARS-CoV-2 S protein attachment and S protein-mediated pseudotyped virus entry into epithelial cells. Therefore, the last set of experiments assessed whether OM-85 treatment also suppressed epithelial cell infection with live SARS-CoV-2. To this end, kidney-derived Vero cells were pretreated with PBS or OM-85 (0.24 to 1.92 mg/ml) for 72 or 96 hours and then incubated for 2 hours with SARS-CoV-2 (isolate USA-WA1/2020). Numbers of pfus/well were counted four days later (**Fig. 7A**). SARS-CoV-2 infection was strongly and significantly inhibited in cultures pre-treated with OM-85 for 72 hours (**Fig. 7C**) or 96 hours (**Fig. E4**) but not in PBS-pre-treated cultures. Inhibition was evident even at the lowest OM-85 concentration and reflected effects of OM-85 pretreatment on epithelial cells rather than SARS-CoV-2 itself because infection was comparably reduced in cultures that did or did not receive OM-85 during the 2-hour infection period (not shown). SARS-CoV-2 infection of lung-derived Calu-3 cells was also significantly inhibited by a 72-hour pretreatment with OM-85, especially at the highest concentrations of bacterial lysate (**Fig. 7B** and **D**). These results clearly demonstrate that OM-85 inhibits *in vitro* SARS-CoV-2 infection of epithelial cells sourced from distinct tissues.

Journal Pre-proof

Discussion

Bacterial lysates are receiving increasing attention for their ability to act as potent response modulators in immune disorders[27, 28]. Our results demonstrate that OM-85, a standardized lysate of human airway-derived bacterial strains, efficiently inhibits live SARS-CoV-2 infection of epithelial cells derived from distinct tissues. OM-85 interfered with multiple steps in the chain of events leading to SARS-CoV-2 epithelial cell infection: it suppressed SARS-CoV-2 receptor (*ACE2* and *TMPRSS2*) expression, SARS-CoV-2 S1 protein-mediated cell attachment, and SARS-CoV-2 S protein-mediated cell entry. Remarkably, OM-85-dependent inhibition only occurred when the lysate downregulated *ACE2,* which initiates SARS-CoV-2 infection by mediating SARS-CoV-2 S protein attachment to target cells. In combination, these data strongly suggest that decreased transcription of SARS-CoV-2 receptor components, primarily *ACE2*, is an essential mechanism for the inhibition of SARS-CoV-2 epithelial cell infection by OM-85. Further studies are needed to identify the molecular pathways underlying *ACE2* downregulation by OM-85. However, OM-85-dependent inhibition of SARS-CoV-2 infection *in vitro* in isolated epithelial cells points to epithelial-intrinsic effects of the lysate.

Our findings have translational implications because the COVID-19 pandemic is not abating and the therapeutic arsenal against COVID-19 is expanding but remains limited. In addition to corticosteroids[29, 30], biologics that interfere with selected pro-inflammatory pathways (e.g., IL-6, IL-1, Janus kinase inhibitors)[31-33] and anti-SARS-CoV-2 antibodies aimed at disrupting progression of COVID-19 infection[34, 35], current COVID-19 vaccines seek to induce humoral and cellular immune responses against the SARS-CoV-2 S

protein so as to neutralize its ability to latch onto cellular receptors and mediate infection[36, 37]. Despite their remarkable overall efficacy, though, vaccines remain cumbersome to distribute and administer. Moreover, viral variants of concern may emerge that resist or even escape the immunity generated by the current vaccines[11, 37]. Antivirals that could be used against SARS-CoV-2 and future emerging viruses are therefore under intense investigation. Remdesivir, an RNA-dependent RNA polymerase inhibitor, was initially reported to shorten COVID-19 hospitalization times[38] but failed in a large clinical trial examining hospitalized patients[39]. Other interesting drugs with potential anti–SARS-CoV-2 properties have been identified through drug-repurposing screens[40-43], an approach that is becoming increasingly attractive because it involves the use of de-risked compounds, potentially lower development costs, and shorter development timelines[44].

In this context, our current results indicate that OM-85 also deserves active consideration. Indeed, the capacity of OM-85 to suppress multiple steps of SARS-CoV-2 cell infection by downregulating the receptor machinery in the epithelium, a primary viral target, may be leveraged to prevent infection and/or decrease its severity by limiting the infection/re-infection cycle. Further studies are needed to better understand the impact of OM-85 on ACE2- and TMPRSS2-expressing primary cells from distinct portions of the airways and from other SARS-CoV-2 target organs. The administration route resulting in optimal inhibition of SARS-CoV-2 infection *in vivo* also remains to be established. However, it is noteworthy that OM-85-induced SARS-CoV-2 receptor downregulation would be expected to protect against multiple SARS-CoV-2 variants and even against other coronaviruses that rely on ACE2 for host cell infection. The

449 impeccable safety profile of OM-85 demonstrated by decades of clinical use as an
450 immunomodulator[14, 45], the lack of reported side effects on ACE2 physiologic
451 functions[14], and the ease of administration of this agent suggest that this standardized
452 bacterial extract may eventually complement the current COVID-19 therapeutic toolkit.

453

Journal Pre-proof

REFERENCES

1. Coronaviridae Study Group of the International Committee on Taxonomy of V. The species Severe acute respiratory syndrome-related coronavirus: classifying 2019-nCoV and naming it SARS-CoV-2. Nat Microbiol. 2020;5(4):536-44.
2. Zhu N, Zhang D, Wang W, Li X, Yang B, Song J, et al. A novel coronavirus from patients with pneumonia in China, 2019. N Engl J Med. 2020;382(8):727-33.
3. Hoffmann M, Kleine-Weber H, Schroeder S, Kruger N, Herrler T, Erichsen S, et al. SARS-CoV-2 cell entry depends on ACE2 and TMPRSS2 and is blocked by a clinically proven protease inhibitor. Cell. 2020;181(2):271-80 e8.
4. Walls AC, Park YJ, Tortorici MA, Wall A, McGuire AT, Veesler D. Structure, function, and antigenicity of the SARS-CoV-2 spike glycoprotein. Cell. 2020;183(6):1735.
5. Wrapp D, Wang N, Corbett KS, Goldsmith JA, Hsieh CL, Abiona O, et al. Cryo-EM structure of the 2019-nCoV spike in the prefusion conformation. Science. 2020;367(6483):1260-3.
6. Kimura H, Francisco D, Conway M, Martinez FD, Vercelli D, Polverino F, et al. Type 2 inflammation modulates ACE2 and TMPRSS2 in airway epithelial cells. J Allergy Clin Immunol. 2020;146(1):80-8 e8.
7. Sungnak W, Huang N, Becavin C, Berg M, Queen R, Litvinukova M, et al. SARS-CoV-2 entry factors are highly expressed in nasal epithelial cells together with innate immune genes. Nat Med. 2020;26(5):681-7.
8. van Doremalen N, Bushmaker T, Morris DH, Holbrook MG, Gamble A, Williamson BN, et al. Aerosol and surface stability of SARS-CoV-2 as compared with SARS-CoV-1. N Engl J Med. 2020;382(16):1564-7.
9. Cheung KS, Hung IFN, Chan PPY, Lung KC, Tso E, Liu R, et al. Gastrointestinal manifestations of SARS-CoV-2 infection and virus load in fecal samples from a Hong Kong cohort: Systematic review and meta-analysis. Gastroenterology. 2020;159(1):81-95.
10. Puelles VG, Lutgehetmann M, Lindenmeyer MT, Sperhake JP, Wong MN, Allweiss L, et al. Multiorgan and renal tropism of SARS-CoV-2. N Engl J Med. 2020;383(6):590-2.
11. Krause PR, Fleming TR, Longini IM, Peto R, Briand S, Heymann DL, et al. SARS-CoV-2 variants and vaccines. N Engl J Med. 2021;385(2):179-86.
12. Schaad UB, Mutterlein R, Goffin H, Group BV-CS. Immunostimulation with OM-85 in children with recurrent infections of the upper respiratory tract: a double-blind, placebo-controlled multicenter study. Chest. 2002;122(6):2042-9.
13. Gutierrez-Tarango MD, Berber A. Safety and efficacy of two courses of OM-85 BV in the prevention of respiratory tract infections in children during 12 months. Chest. 2001;119(6):1742-8.
14. Esposito S, Soto-Martinez ME, Feleszko W, Jones MH, Shen KL, Schaad UB. Nonspecific immunomodulators for recurrent respiratory tract infections, wheezing and asthma in children: a systematic review of mechanistic and clinical evidence. Curr Opin Allergy Clin Immunol. 2018;18(3):198-209.
15. Pasquali C, Salami O, Taneja M, Gollwitzer ES, Trompette A, Pattaroni C, et al. Enhanced mucosal antibody production and protection against respiratory infections following an orally administered bacterial extract. Front Med (Lausanne). 2014;1:41.

Journal Pre-proof

16. Roth M, Pasquali C, Stolz D, Tamm M. Broncho Vaxom (OM-85) modulates rhinovirus docking proteins on human airway epithelial cells via Erk1/2 mitogen activated protein kinase and cAMP. PLoS One. 2017;12(11):e0188010.
17. Pivniouk V, Gimenes JA, Ezeh P, Michael AN, Pivniouk O, Hahn S, et al. Airway administration of OM-85, a bacterial lysate, blocks experimental asthma by targeting dendritic cells and the epithelium/IL-33/ILC2 axis. J Allergy Clin Immunol. 2021;Sep 22:S0091-6749(21)01403-2. doi: 10.1016/j.jaci.2021.09.013.
18. Kraft M, Adler KB, Ingram JL, Crews AL, Atkinson TP, Cairns CB, et al. Mycoplasma pneumoniae induces airway epithelial cell expression of MUC5AC in asthma. Eur Respir J. 2008;31(1):43-6.
19. Crawford KHD, Eguia R, Dingens AS, Loes AN, Malone KD, Wolf CR, et al. Protocol and reagents for pseudotyping lentiviral particles with SARS-CoV-2 spike protein for neutralization assays. Viruses. 2020;12(5).
20. Sastry L, Johnson T, Hobson MJ, Smucker B, Cornetta K. Titering lentiviral vectors: comparison of DNA, RNA and marker expression methods. Gene Ther. 2002;9(17):1155-62.
21. White SM, Renda M, Nam NY, Klimatcheva E, Zhu Y, Fisk J, et al. Lentivirus vectors using human and simian immunodeficiency virus elements. J Virol. 1999;73(4):2832-40.
22. Ziegler CGK, Allon SJ, Nyquist SK, Mbano IM, Miao VN, Tzouanas CN, et al. SARS-CoV-2 receptor ACE2 is an interferon-stimulated gene in human airway epithelial cells and is detected in specific cell subsets across tissues. Cell. 2020;181(5):1016-35 e19.
23. Johansen MD, Irving A, Montagutelli X, Tate MD, Rudloff I, Nold MF, et al. Animal and translational models of SARS-CoV-2 infection and COVID-19. Mucosal Immunol. 2020;13(6):877-91.
24. Dittmar M, Lee JS, Whig K, Segrist E, Li M, Kamalia B, et al. Drug repurposing screens reveal cell-type-specific entry pathways and FDA-approved drugs active against SARS-Cov-2. Cell Rep. 2021;35(1):108959.
25. Felgenhauer U, Schoen A, Gad HH, Hartmann R, Schaubmar AR, Failing K, et al. Inhibition of SARS-CoV-2 by type I and type III interferons. J Biol Chem. 2020;295(41):13958-64.
26. Hou YJ, Okuda K, Edwards CE, Martinez DR, Asakura T, Dinnon KH, 3rd, et al. SARS-CoV-2 reverse genetics reveals a variable infection gradient in the respiratory tract. Cell. 2020;182(2):429-46 e14.
27. Larenas-Linnemann D, Rodriguez-Perez N, Arias-Cruz A, Blandon-Vijil MV, Del Rio-Navarro BE, Estrada-Cardona A, et al. Enhancing innate immunity against virus in times of COVID-19: Trying to untangle facts from fictions. World Allergy Organ J. 2020;13(11):100476.
28. Suarez N, Ferrara F, Rial A, Dee V, Chabalgoity JA. Bacterial Lysates as Immunotherapies for Respiratory Infections: Methods of Preparation. Front Bioeng Biotechnol. 2020;8:545.
29. Horby P, Lim WS, Emberson JR, Mafham M, Bell JL, Linsell L, et al. Dexamethasone in hospitalized patients with Covid-19. N Engl J Med. 2021;384(8):693-704.
30. Ramakrishnan S, Nicolau DV, Jr., Langford B, Mahdi M, Jeffers H, Mwasuku C, et al. Inhaled budesonide in the treatment of early COVID-19 (STOIC): a phase 2, open-label, randomised controlled trial. Lancet Respir Med. 2021.
31. Rubin EJ, Longo DL, Baden LR. Interleukin-6 receptor inhibition in Covid-19 - Cooling the inflammatory soup. N Engl J Med. 2021.

Journal Pre-proof

32. Pontali E, Volpi S, Signori A, Antonucci G, Castellaneta M, Buzzi D, et al. Efficacy of early anti-inflammatory treatment with high doses of intravenous anakinra with or without glucocorticoids in patients with severe COVID-19 pneumonia. J Allergy Clin Immunol. 2021;147(4):1217-25.
33. Guimaraes PO, Quirk D, Furtado RH, Maia LN, Saraiva JF, Antunes MO, et al. Tofacitinib in patients hospitalized with Covid-19 pneumonia. N Engl J Med. 2021;385(5):406-15.
34. Cohen MS. Monoclonal antibodies to disrupt progression of early Covid-19 infection. N Engl J Med. 2021;384(3):289-91.
35. Dougan M, Nirula A, Azizad M, Mocherla B, Gottlieb RL, Chen P, et al. Bamlanivimab plus Etesevimab in Mild or Moderate Covid-19. N Engl J Med. 2021.
36. Kyriakidis NC, Lopez-Cortes A, Gonzalez EV, Grimaldos AB, Prado EO. SARS-CoV-2 vaccines strategies: a comprehensive review of phase 3 candidates. NPJ Vaccines. 2021;6(1):28.
37. COVID-19 Vaccine Resource Center. N Engl J Med.https://www-nejm-org.ezproxy2.library.arizona.edu/covid-vaccine.
38. Pardo J, Shukla AM, Chamarthi G, Gupte A. The journey of remdesivir: from Ebola to COVID-19. Drugs Context. 2020;9.
39. Beigel JH, Tomashek KM, Dodd LE, Mehta AK, Zingman BS, Kalil AC, et al. Remdesivir for the treatment of Covid-19 - Final report. N Engl J Med. 2020;383(19):1813-26.
40. Gordon DE, Jang GM, Bouhaddou M, Xu J, Obernier K, White KM, et al. A SARS-CoV-2 protein interaction map reveals targets for drug repurposing. Nature. 2020;583(7816):459-68.
41. Riva L, Yuan S, Yin X, Martin-Sancho L, Matsunaga N, Pache L, et al. Discovery of SARS-CoV-2 antiviral drugs through large-scale compound repurposing. Nature. 2020;586(7827):113-9.
42. Drayman N, DeMarco JK, Jones KA, Azizi SA, Froggatt HM, Tan K, et al. Masitinib is a broad coronavirus 3CL inhibitor that blocks replication of SARS-CoV-2. Science. 2021;373(6557):931-6.
43. Mahoney M, Damalanka VC, Tartell MA, Chung DH, Lourenco AL, Pwee D, et al. A novel class of TMPRSS2 inhibitors potently block SARS-CoV-2 and MERS-CoV viral entry and protect human epithelial lung cells. Proc Natl Acad Sci U S A. 2021;118(43).
44. Pushpakom S, Iorio F, Eyers PA, Escott KJ, Hopper S, Wells A, et al. Drug repurposing: progress, challenges and recommendations. Nat Rev Drug Discov. 2019;18(1):41-58.
45. Cao C, Wang J, Li Y, Li Y, Ma L, Abdelrahim MEA, et al. Efficacy and safety of OM-85 in paediatric recurrent respiratory tract infections which could have a possible protective effect on COVID-19 pandemic: A meta-analysis. Int J Clin Pract. 2021;75(5):e13981.

579 **LEGENDS**

580 **Figure 1. *OM-85 inhibits Ace2 and Tmprss2 transcription in the mouse lung*.** (**A**)
581 Balb/c mice were treated i.n. with OM-85 (1 mg in 50 μl) 14 times as indicated in the
582 chart (T_1-T_{14}). The last OM-85 treatment was administered at day 32. Lungs for
583 transcriptional analyses were collected 2 (day 34) or 7 (day 39) days later. (**B**) *Ace2* and
584 *Tmprss2* mRNA levels in the lungs of mice treated i.n. with OM-85 (1 mg/treatment x 14
585 treatments) or PBS (n=6/group) over 32 days and sacrificed at day 39. Data were
586 extracted from DESeq2-normalized RNA-Seq counts after adjusting for latent factors. P-
587 values were calculated from differential expression analysis (DESeq2 Wald test). (**C-D**)
588 *Ace2* and *Tmprss2* expression in the lungs of Balb/c mice treated i.n. with OM-85 or
589 PBS as in panel A was measured by RT-qPCR at day 34 or 39 (i.e., 2 or 7 days after
590 the last OM-85 treatment, respectively; n=9-10 mice/group at day 2, and n=7-8
591 mice/group at day 7). mRNA levels normalized by *Gapdh* are shown relative to PBS. A
592 Wilcoxon two-sample test was used for statistical analysis after testing for normality of
593 sample distribution.

594 **Figure 2. *OM-85 inhibits ACE2 and TMPRSS2 transcription in NHP and human***
595 ***epithelial cell lines from kidney and lung***. *ACE2* (**A,C**) and *TMPRSS2* (**B,D**) mRNA
596 levels were measured by RT-qPCR in Vero E6 (**A,B**) and Calu-3 (**C,D**) epithelial cells
597 treated with OM-85 (0.48 mg/ml) or PBS for 24-96 hr. mRNA levels at each time point
598 were normalized by *GAPDH* and are shown relative to PBS. Data are from two pooled
599 experiments (**A,C**) and one representative experiment out of two (**B,D**) (n=3-4
600 wells/condition, each run in triplicate). An unpaired, two-tailed *t* test (**A,B,C**) or a

Journal Pre-proof

Wilcoxon two-sample test (**D**) were used for statistical analysis after testing for normality of sample distribution.

Figure 3*. OM-5 inhibits ACE2 and TMPRSS2 transcription in primary normal human bronchial epithelial cells.* Bronchial epithelial cells freshly isolated from a healthy donor were cultured to confluence and differentiated onto collagen-coated polyester 12-mm Transwell™ insert membranes for 2 weeks at air–liquid interface. Cells were then stimulated apically with PBS or OM-85 (1.92 mg/ml) for 48 or 72 hours. *ACE2* and *TMPRSS2* expression was determined by RT-qPCR (n=3 wells/condition, each run in triplicate). mRNA levels at each time point were normalized by *GAPDH* and are shown relative to PBS. An unpaired, two-tailed *t* test was used for statistical analysis after assessing the normality of sample distribution.

Figure 4. ***OM-5 downregulates surface ACE2 protein expression in epithelial cells.*** Vero E6 **(A-C)** and Calu-3 **(D-F)** cells were treated with OM-85 (0.48 or 1.92 mg/ml) for 72 hours and assessed for ACE2 protein expression by flow cytometry with ACE2-specific monoclonal antibodies and relevant isotype controls. **A**, **D**: representative ACE2 flow cytometry plots (shaded area: isotype control; thin line: PBS-treated cells; thick line: cells treated with OM-85, 1.92 mg/ml); **B**, **E:** ACE2 MFI and percentages of $ACE2^+$ cells in PBS- and OM-85-treated cells (**C** and **F**). Data are from one experiment with four samples/condition. An unpaired, two-tailed *t* test was used for statistical analysis after testing for normality of sample distribution.

Figure 5. *OM-85 reduces S1 protein-mediated attachment to epithelial cells*. Representative flow cytometry plots showing SARS-CoV-2 S1 protein binding to

parental HEK293T cells and HEK293T cells stably transfected with human *ACE2* (ACE2/HEK293T) (**A**), Vero E6 and Calu-3 (**B**) epithelial cells. Cells were treated with PBS or OM-85 (1.92 mg/ml) for 72 hours and then incubated with or without recombinant His-tagged S1 protein, followed by an anti-His-PE antibody. S1 binding was assessed by flow cytometry. **(C)** Effects of OM-85 on S1 protein binding to Vero E6 or Calu-3 cells. Data are shown as percentages of S1 protein-binding cells in OM-85-treated versus PBS-treated cultures [n=5-6 wells/group from three (Vero E6 cells) or two (Calu-3 cells) independent experiments]. An unpaired, two-tailed *t* test was used for statistical analysis after testing for normality of sample distribution.

Figure 6*. OM-85 inhibits entry of S protein-pseudotyped lentiviral particles into Vero E6 cells.* **A.** Vero E6 cells were treated with OM-85 (0.48 mg/ml) or PBS for 48 hours, washed and transduced with lentiviral particles that were pseudotyped with SARS-CoV-2 S protein ($0.2x10^4$ TU) or VSV-G protein ($2x10^4$ TU) and carried a GFP reporter. Shown are frames representative of GFP immunofluorescence under various experimental conditions. (**B-E**) GFP fluorescence was assessed under a microscope (10X magnification) 72 hours post transduction and quantified using the Slide Analyzer software in Vero E6 (**B,C**) and ACE2/HEK293T (**D,E**) cells transduced with either SARS-CoV-2-S-pseudotyped virus (**B,D**) or VSV-G-pseudotyped virus (**C,E**). Results represent the average $\pm$ SEM of 20 (SARS-CoV-2-S-pseudotyped virus) or 10 (VSV-G-pseudotyped virus) random frames from one representative experiment out of two independent experiments. A Wilcoxon two-sample test was used for statistical analysis after assessing the normality of sample distribution.

Journal Pre-proof

Figure 7. ***OM-5 inhibits epithelial cell infection by SARS-CoV-2.*** **A**: Vero cells were pretreated with PBS or OM-85 (0.24 to 1.92 mg/ml) for a total of 72 hours and then infected with SARS-CoV-2 (isolate USA-WA1/2020, 15 pfu/well) for 2 hours. Plaques were counted as described in Methods. **B:** Calu-3 cells treated with PBS or OM-85 (0.24-1.92 mg/ml) for 72 hours were infected with SARS-CoV-2 (WA/2020, ~100 pfus) for 2 hours. Cells were then cultured for 48 hours in medium containing the original OM-85 concentrations. Viral titers were determined by dispensing 10-fold serial dilutions of Calu-3 culture supernatants on 96-well indicator Vero plates. Plaques were counted as described in Methods. The number of pfus/well of Calu-3 plates was calculated by dividing the number of plaques on indicator Vero plates by the dilution factor. Shown are average numbers ± SEM of pfus detected in four (**C**) or eight (**D**) SARS-CoV-2-infected replicate wells pretreated with PBS or increasing OM-85 concentrations. Data were pooled from two independent experiments (**A, C**) and one representative experiment (**B, D**). A two-tailed *t* test was used for statistical analysis after assessing the normality of sample distribution.

Journal Pre-proof

AUTHOR CONTRIBUTIONS

VP and DV designed the study. Advice about selected models was provided by JMC, MK and JNZ. Data were acquired by VP, OP, JLU, ANM, SRH, MYC, SH, SPM and PE and analyzed by VP, ADV, DP and DV. VP and DV drafted the article. All authors approved the final version of the manuscript. DV was responsible for the integrity of the work.

Journal Pre-proof

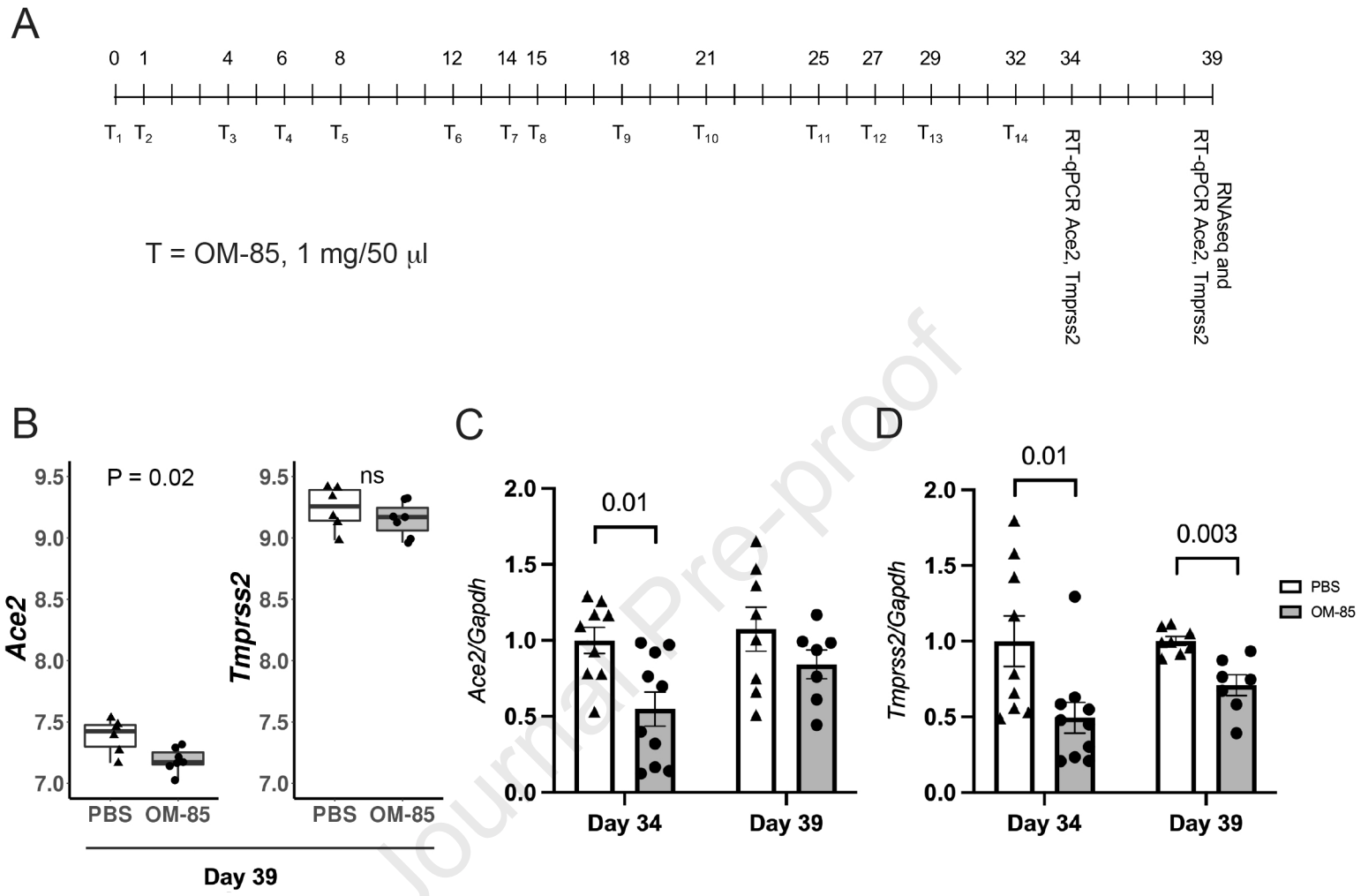

Journal Pre-proof

Figure 1

Journal Pre-proof

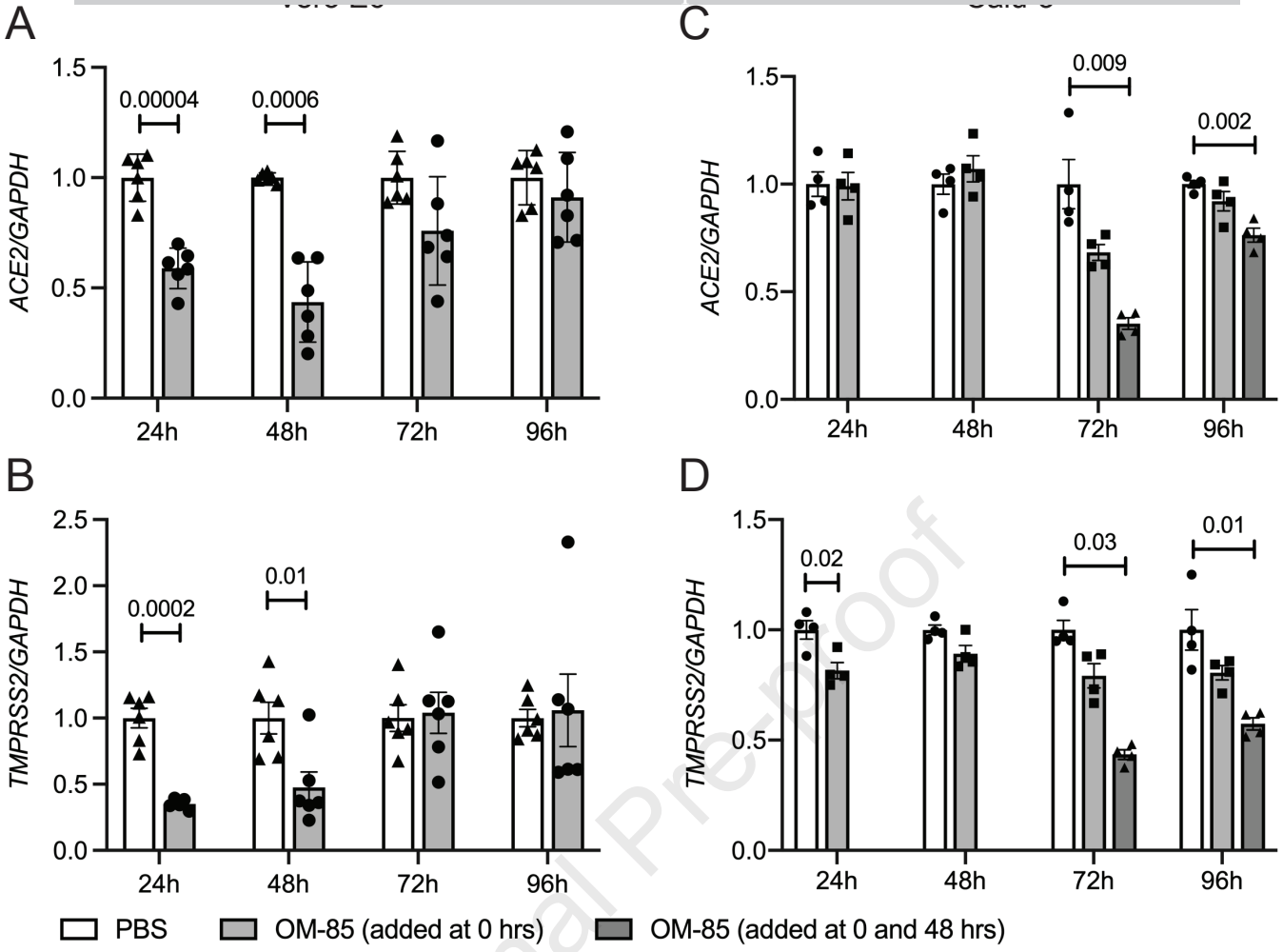

Journal Pre-proof

Figure 2

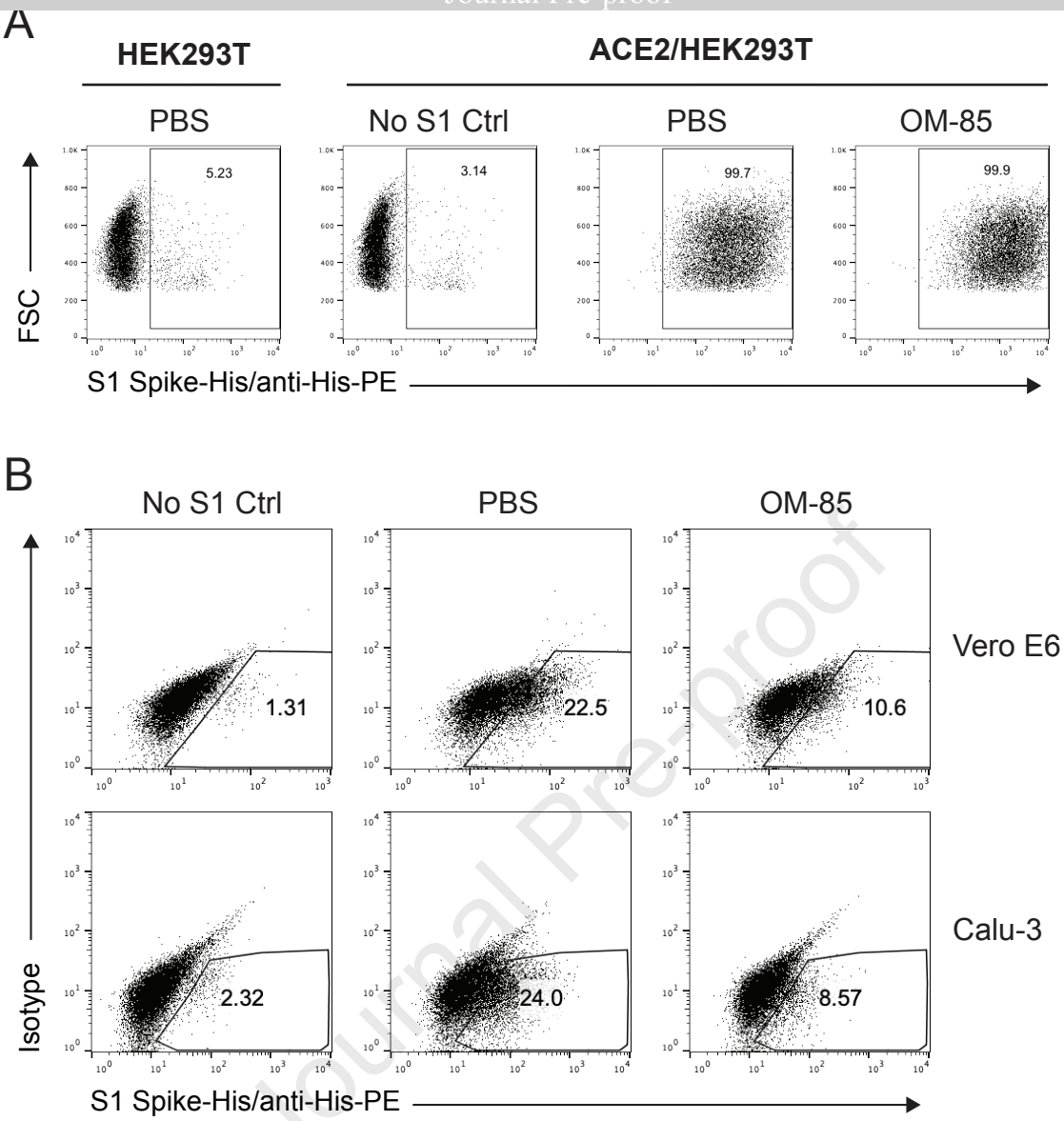

Journal Pre-proof

Figure 5

Journal Pre-proof

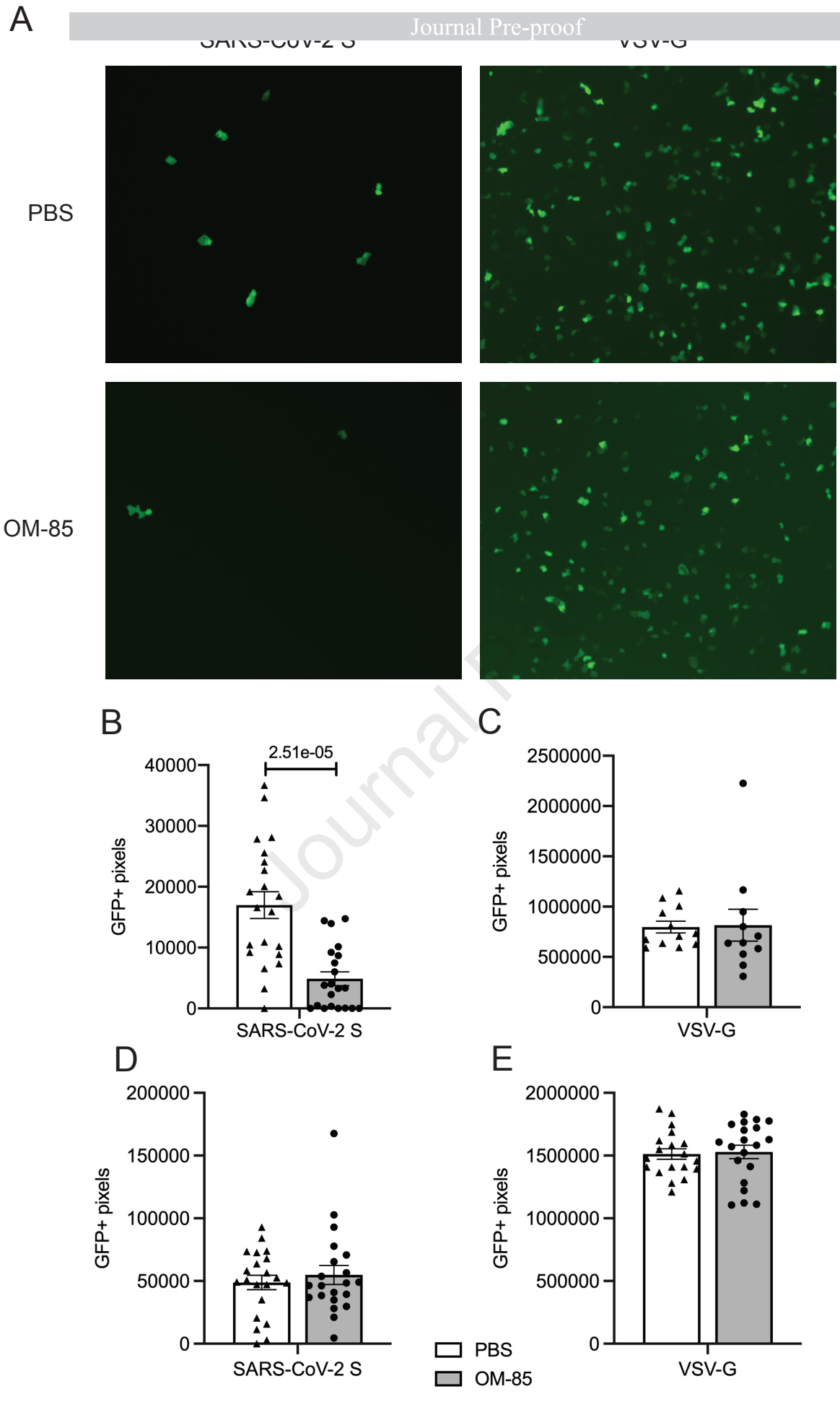

Figure 6

Journal Pre-proof

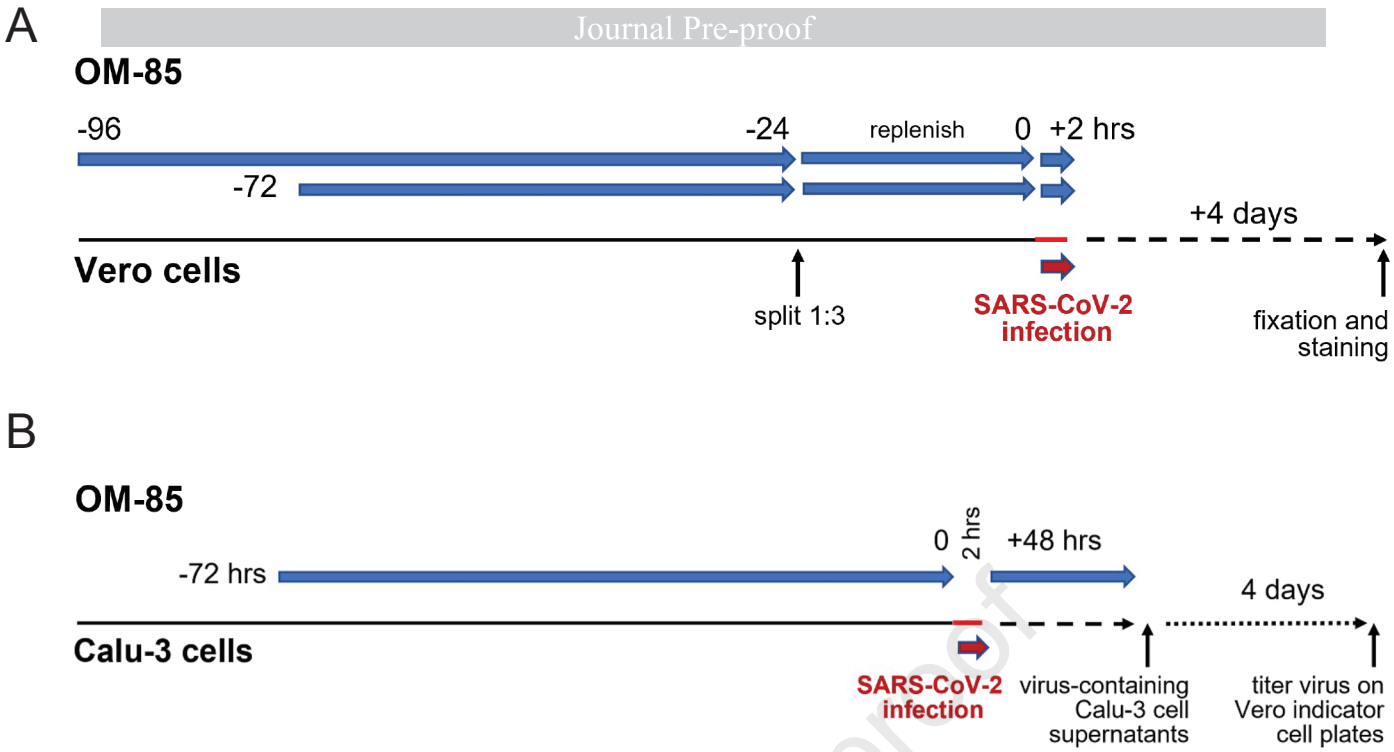

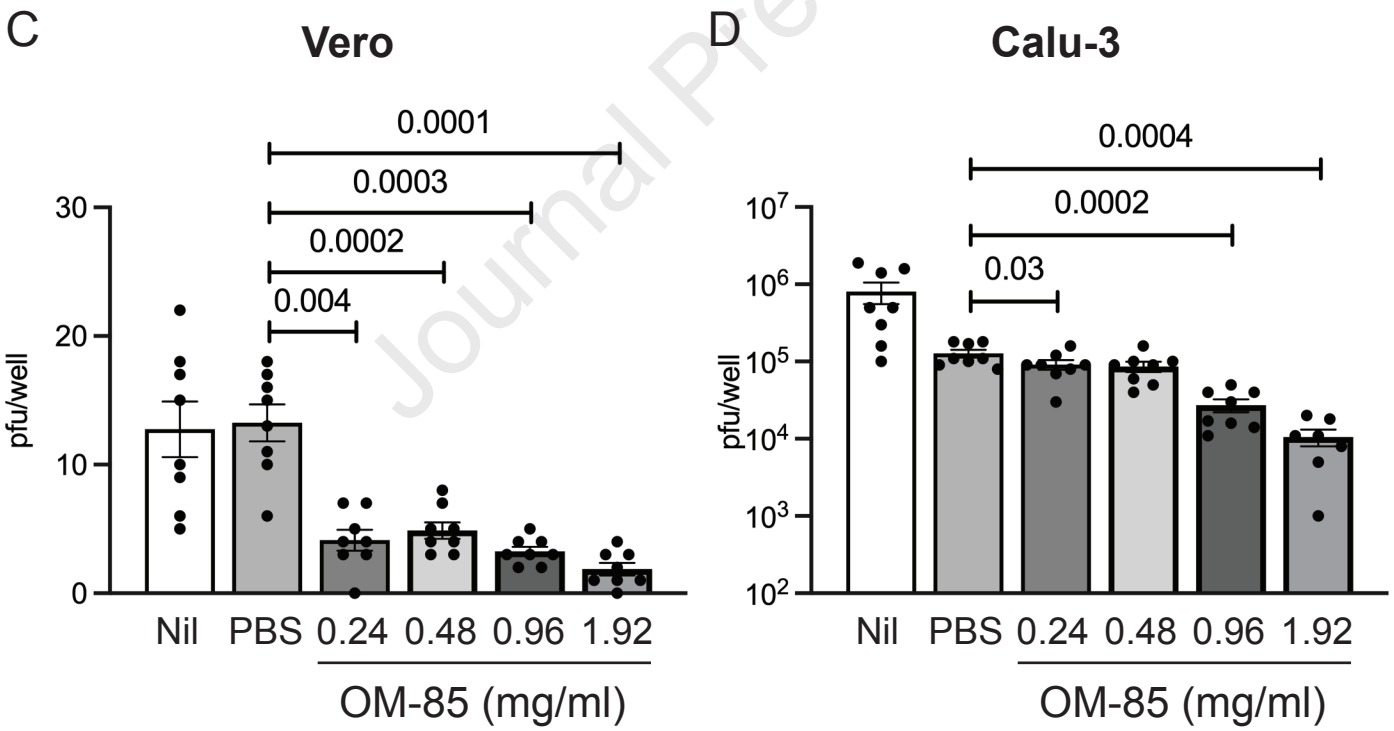

Figure 7

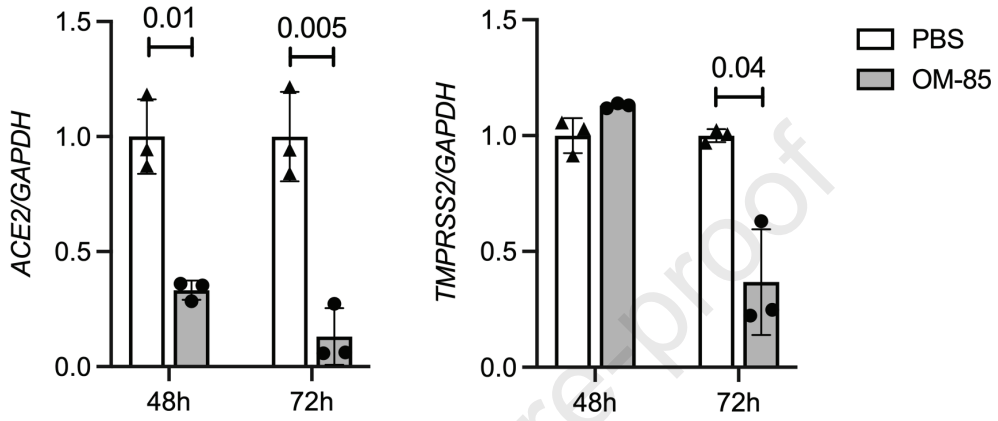

Journal Pre-proof

Figure 3

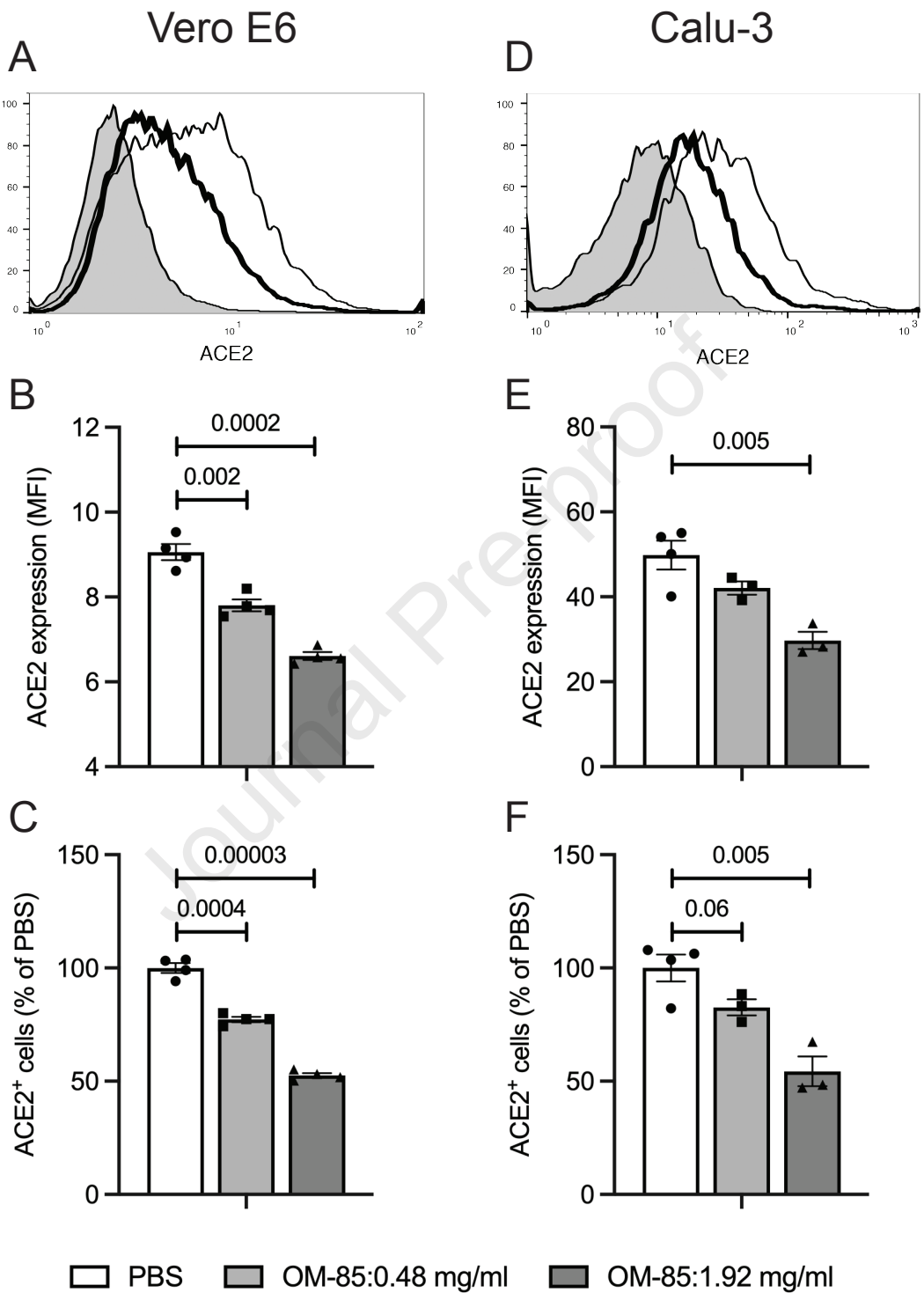

Figure 4

Journal Pre-proof

	PBS	OM-85
ACE2/HEK293T	99.3±0.3	99.4±0.1

Table E.1: Effect of OM-85 on human ACE2 expression by ACE2/HEK293T cells. Cells were treated with PBS or OM-85 (1.92 mg/ml) for 72 hours, and human ACE2 expression was evaluated by flow cytometry with an AF647-conjugated anti-human ACE2 antibody or isotype control. Data are shown as mean percentages ± SE of ACE2-positive cells in PBS- or OM-85-treated cultures (n=3/condition). Negligible proportions of positive cells were detected in the isotype control samples.

Journal Pre-proof

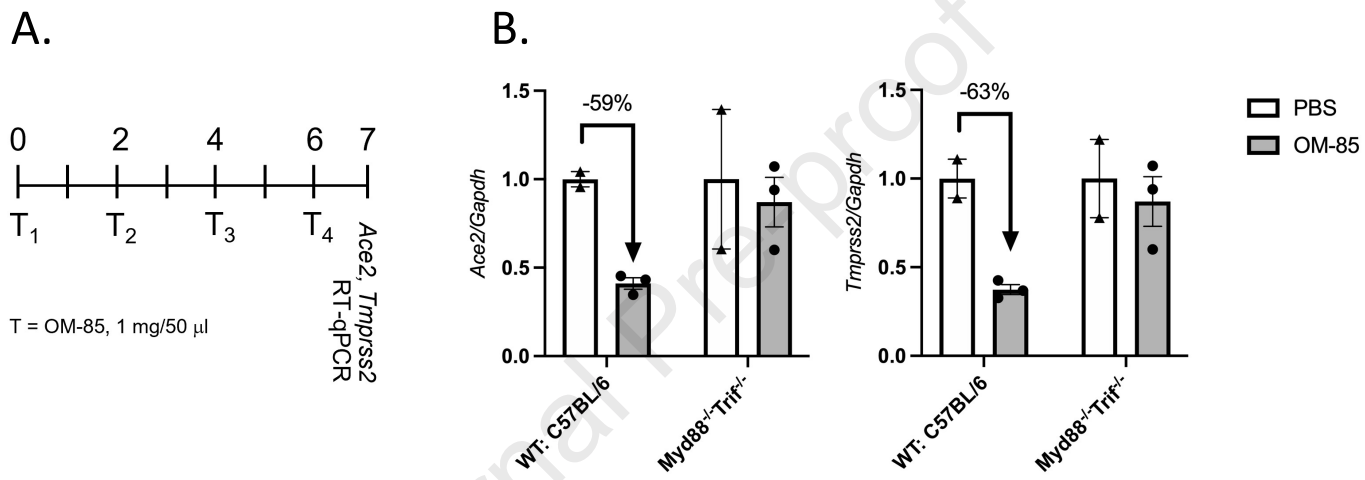

Figure E1. OM-85-induced downregulation of *Ace2* and *Tmprss2* in the mouse lung is *Myd88/Trif*-dependent

Journal Pre-proof

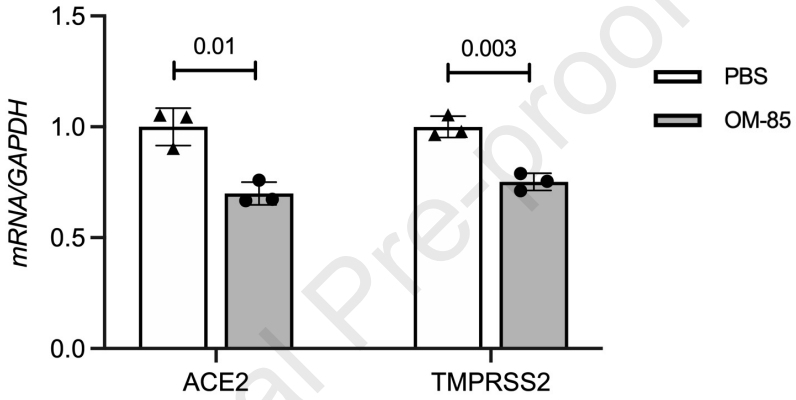

Figure E2. OM-85 inhibits ACE2 and TMPRSS2 transcription in human colon Caco-2 cells.

Journal Pre-proof

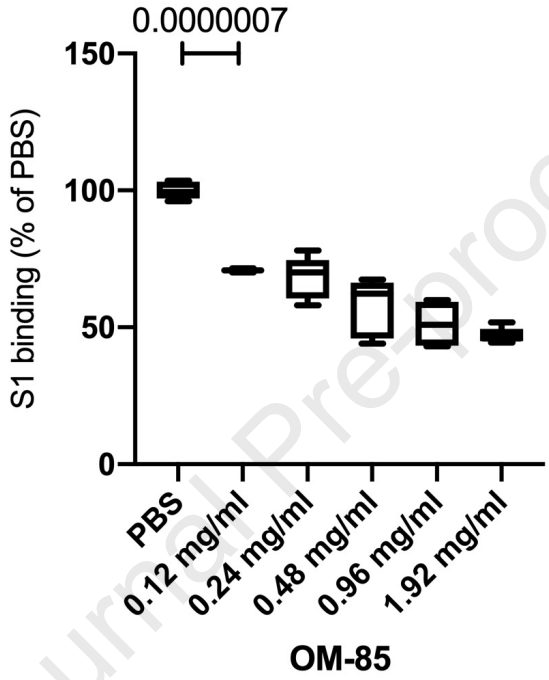

Journal Pre-proof

Figure E3. OM-85 dose-dependently inhibits S1 protein binding to Vero E6 cells.

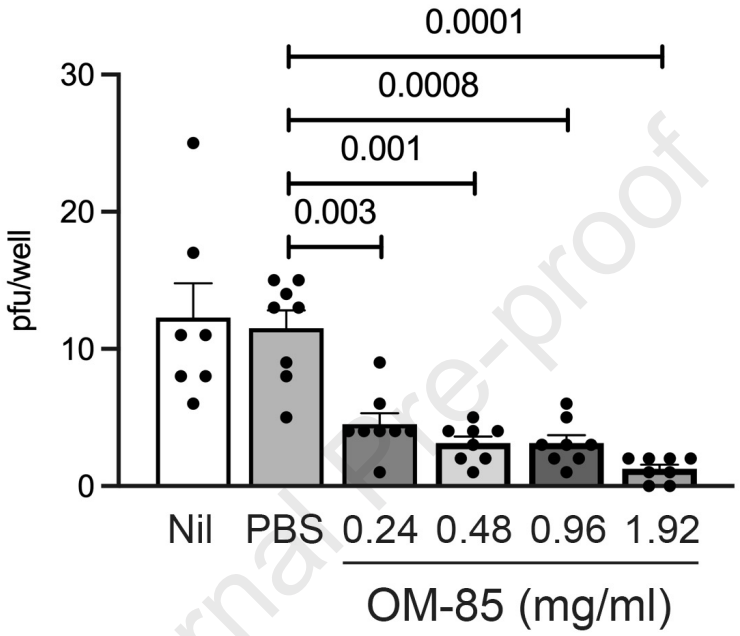

Journal Pre-proof

Figure E4. A 96-hour pre-treatment with OM-85 inhibits Vero cell infection by SARS-CoV-2.

ONLINE SUPPLEMENTAL MATERIAL

Mice OM-85 (1 mg in 50 µl, 25 µl/nostril) was instilled i.n. every 2-3 days (14 times total) beginning at day 0 (**Fig. 1A**) into adult (6–7-week-old) male Balb/c mice (Charles Rivers Laboratories, Wilmington, MA) maintained on a standard hypoallergenic diet under specific pathogen-free conditions. In selected experiments, OM-85 (1 mg in 50 µl) was instilled i.n. four times into 8-week-old WT C57BL/6 mice (Charles Rivers Laboratories) or *Myd88*$^{-/-}$*Trif*$^{-/-}$ C57BL/6 mice (kindly provided by Dominik Schenten, University of Arizona). Lungs were collected and preserved in RNAlater (Qiagen, Germantown, MD). All animal procedures conform to the principles set forth by the Animal Welfare Act and the National Institutes of Health guidelines for the care and use of laboratory animals in biomedical research and were approved by the University of Arizona Institutional Animal Care and Use Committee.

OM-85 OM-85 concentrate was provided by OM Pharma and is the soluble supernatant obtained after bacterial lysis. It represents the drug substance prior to its lyophilization and final manufacturing as Broncho-Vaxom^{TM}. OM-85 lots # 1618006 (22.9 mg/ml of dry residue) and 1620074 (23.1 mg/ml of dry residue) were used in these experiments.

RNA-sequencing from mouse lung tissue Balb/c mice were treated with OM-85 or PBS as depicted in **Fig. 1A**. Unfractionated lung tissue was collected at day 39 and processed for RNA-sequencing. Raw and normalized data for the complete dataset were deposited in the GEO database (GSE167867), where detailed information on data processing and normalization can be found. Briefly, RNA-seq reads (>25 bp after

Journal Pre-proof

trimming adapter sequences) were mapped to the BALB/cJ genome (version mm10) using STAR[1], and genomic coordinates were shifted to the standard mm10 genome using MARGE (http://cistrome.org/MARGE/index. html). Uniquely aligning reads were used to generate gene counts relying on HOMER (http://homer.ucsd.edu/homer/index.html). Latent factors potentially introducing unwanted variation were removed using RUVSeq[2]. Data for *Ace2* and *Tmprss2* expression in OM-85- and PBS-treated mice were extracted from DESeq2-normalized counts[3], and P-values from differential expression analysis (DESeq2) were reported. P-values < 0.05 were considered significant.

RNA extraction, cDNA synthesis and RT-qPCR RNA from cell lines or mouse lung tissue was extracted with the RNeasy kit (Qiagen, Germantown, MD). After extraction, total RNA (500 ng) was used as a template to synthesize cDNA with the QuantiTect Reverse Transcription Kit (Qiagen). RT-qPCR was carried out using the QuantiTect SYBR Green PCR kit (Qiagen) on an ABI 7900 Applied Biosystems thermocycler (ThermoFisher Scientific). All genes except African green monkey *(Chlorocebus sabaeus) TMPRSS2* were amplified using commercially available primers (QuantiTect Primer Assays, Qiagen). For green monkey *TMPRSS2,* the following primers were used: TGCATCAGCTCCTCTAACTG (forward) and GAGATGAGTACACCTGAAGG (reverse). Each sample was run in triplicate. The change in gene expression relative to PBS was normalized to glyceraldehyde 3-phosphate dehydrogenase *(Gapdh)* and calculated using the $2^{-\Delta\Delta ct}$ method[4].

Flow cytometry evaluation of ACE2 expression Vero E6 and Calu-3 cells were grown in 12-well plates until confluent and treated with OM-85 (0.48 or 1.92 mg/ml) or

Journal Pre-proof

PBS. After 72 hours, cells were harvested, and a single cell suspension was prepared in FACSWash buffer (PBS with 1% BSA and 0.1% NaN_3) at 0.5-1x10^7 cells/ml. To block nonspecific staining, cells were incubated on ice for 10 min in the same buffer containing normal mouse serum (5%) followed by a 30 min incubation with either mouse anti-human ACE2-PE (Sino Biological, clone 36[5, 6], for Vero E6 cells), or mouse anti-human ACE2-AF647 (R&D Systems, Minneapolis, MN: clone 535919[7-11], for Calu-3 cells). We further validated the ACE2-specificity of these monoclonal antibodies by showing that they detected >99% of ACE2-transfected HEK293T cells, but <1% of parental, untransfected HEK293T cells. 20,000-30,000 events were acquired on a FACSCalibur flow cytometer (BD Biosciences) and analyzed using FlowJo software (Version 10.6.0, Becton Dickinson, 2019).

Statistical analyses Statistical differences between treatment groups were assessed by an unpaired, two-tailed *t* test or a Wilcoxon two-sample test after assessing the normality of sample distribution using the Shapiro-Wilk test. P values <0.05 were considered statistically significant. Analyses were conducted in Stata (version 14.2), R (version 3.5.0), GraphPad Prism (version 9.1.1) and Microsoft Excel.

Journal Pre-proof

SUPPLEMENTAL REFERENCES

1. Dobin A, Davis CA, Schlesinger F, Drenkow J, Zaleski C, Jha S, et al. STAR: ultrafast universal RNA-seq aligner. Bioinformatics. 2013;29(1):15-21.

2. Risso D, Ngai J, Speed TP, Dudoit S. Normalization of RNA-seq data using factor analysis of control genes or samples. Nat Biotechnol. 2014;32(9):896-902.

3. Love MI, Huber W, Anders S. Moderated estimation of fold change and dispersion for RNA-seq data with DESeq2. Genome Biol. 2014;15(12):550.

4. Livak KJ, Schmittgen TD. Analysis of relative gene expression data using real-time quantitative PCR and the 2(-Delta Delta C(T)) Method. Methods. 2001;25(4):402-8.

5. Wang C, Wang S, Chen Y, Zhao J, Han S, Zhao G, et al. Membrane Nanoparticles Derived from ACE2-Rich Cells Block SARS-CoV-2 Infection. ACS Nano. 2021;15(4):6340-51.

6. Li J, Zou W, Yu K, Liu B, Liang W, Wang L, et al. Discovery of the natural product 3',4',7,8-tetrahydroxyflavone as a novel and potent selective BRD4 bromodomain 2 inhibitor. J Enzyme Inhib Med Chem. 2021;36(1):903-13.

7. Zhang Q, Bastard P, Liu Z, Le Pen J, Moncada-Velez M, Chen J, et al. Inborn errors of type I IFN immunity in patients with life-threatening COVID-19. Science. 2020;370(6515).

8. Xu C, Wang A, Geng K, Honnen W, Wang X, Bruiners N, et al. Human Immunodeficiency Viruses Pseudotyped with SARS-CoV-2 Spike Proteins Infect a Broad Spectrum of Human Cell Lines through Multiple Entry Mechanisms. Viruses. 2021;13(6).

9. Neises JZ, Hossain MS, Sultana R, Wanniarachchi KN, Wollman JW, Nelson E, et al. Seroprevalence of SARS-CoV-2 antibodies among rural healthcare workers. J Med Virol. 2021;93(12):6611-8.

10. Lu Q, Liu J, Zhao S, Gomez Castro MF, Laurent-Rolle M, Dong J, et al. SARS-CoV-2 exacerbates proinflammatory responses in myeloid cells through C-type lectin receptors and Tweety family member 2. Immunity. 2021;54(6):1304-19 e9.

11. Liu Y, Soh WT, Kishikawa JI, Hirose M, Nakayama EE, Li S, et al. An infectivity-enhancing site on the SARS-CoV-2 spike protein targeted by antibodies. Cell. 2021;184(13):3452-66 e18.

Journal Pre-proof

Supplemental figure legends

Figure E1. OM-85-induced downregulation of *Ace2* and *Tmprss2* in the mouse lung is *Myd88/Trif*-dependent. (**A**) WT and *Myd88*$^{-/-}$*Trif*$^{-/-}$ C57BL/6 mice were treated i.n. with OM-85 (1 mg in 50 μl) or PBS every 2 days for four times as indicated in the chart (T_1-T_4). Lung cells for transcriptional analyses were collected at day 7. (**B**) *Ace2* and *Tmprss2* mRNA levels in the lungs of WT and *Myd88*$^{-/-}$*Trif*$^{-/-}$ C57BL/6 mice treated i.n. with OM-85 or PBS were measured by RT-qPCR and normalized by *Gapdh* (n=2 mice each/PBS group, and n=3 mice each/OM-85 group).

Figure E2. *OM-85 inhibits ACE2 and TMPRSS2 transcription in human colon Caco-2 cells*. *ACE2* and *TMPRSS2* expression was measured by RT-qPCR in cells treated with OM-85 (0.48 mg/ml) or PBS for 48 hrs. mRNA levels were normalized by *GAPDH* and are shown relative to PBS. Data are from one representative experiment (n=3-4 wells/condition, each run in triplicate) out of two. An unpaired, two-tailed *t* test was used for statistical analysis after testing for normality of sample distribution.

Figure E3. *OM-85 dose-dependently inhibits S1 protein binding to Vero E6 cells*. Cells were treated with PBS or increasing OM-85 concentrations for 72 hours and then incubated with or without recombinant His-tagged S1 protein, followed by an anti-His-PE antibody. S1 binding was assessed by flow cytometry. Data are shown as percentages of S1 protein-binding cells in OM-85-treated versus PBS-treated cultures (n=5-6 wells/group). An unpaired, two-tailed *t* test was used for statistical analysis after testing for normality of sample distribution.

Figure E4. ***A 96-hour pre-treatment with OM-85 inhibits Vero cell infection by***

Journal Pre-proof

SARS-CoV-2. Vero cells were pretreated with PBS or OM-85 (0.24 to 1.92 mg/ml) for 96 hours and then infected with SARS-CoV-2 (isolate USA-WA1/2020, 15 pfu/well) for 2 hours. Plaques were counted as described in Methods. Shown are average numbers ± SEM of pfu detected in eight SARS-CoV-2-infected replicate wells pretreated with PBS or increasing OM-85 concentrations. Data were pooled from two independent experiments. A two-tailed *t* test was used for statistical analysis after assessing the normality of sample distribution.

Journal Pre-proof